arXiv:1409.1703v1 [quant-ph] 5 Sep 2014

Phase-noise protection in quantum-enhanced differential interferometry

M. Landini[1,2], M. Fattori[1,2,3], L. Pezzè[1,2,4] and A. Smerzi[1,2,4]

[1]Istituto Nazionale di Ottica-CNR (INO-CNR), Via Nello Carrara 1, I-50019 Sesto Fiorentino, Italy

[2]European Laboratory for Non-Linear Spectroscopy (LENS) and Dipartimento di Fisica, Universitá di Firenze, Via Nello Carrara 1, I-50019 Sesto Fiorentino, Italy

[3]Istituto Nazionale di Fisica Nucleare (INFN), Sezione di Firenze, Via Sansone 1, I-50019 Sesto Fiorentino, Italy

[4]QSTAR, Largo Enrico Fermi 2, 50125 Firenze, Italy

E-mail: `luca.pezze@ino.it`

Abstract. Differential interferometry (DI) with two coupled sensors is a most powerful approach for precision measurements in presence of strong phase noise. However DI has been studied and implemented only with classical resources. Here we generalize the theory of differential interferometry to the case of entangled probe states. We demonstrate that, for perfectly correlated interferometers and in the presence of arbitrary large phase noise, sub-shot noise sensitivities – up to the Heisenberg limit – are still possible with a special class of entangled states in the ideal lossless scenario. These states belong to a decoherence free subspace where entanglement is passively protected. Our work pave the way to the full exploitation of entanglement in precision measurements in presence of strong phase noise.

PACS numbers: 03.75.Dg; 42.50.Sc; 42.50.Lc 03.75.Gg;

1. Introduction

Atom interferometers [1] offer nowadays unprecedented precision in the measurement of gravity [2], inertial forces [3], atomic properties [4] and fundamental constants [5]. Their large sensitivity makes almost unavoidable their coupling to the environment which mainly results in a random noise which affects the signal phase. In order to overcome this limitation, many experiments aiming at precision measurements adopt a differential scheme: two interferometers operating in parallel are affected by the same phase noise and accumulate a different phase shift induced by the measured field. Estimation of the differential phase allows high resolution thanks to noise cancellation [6]. Schemes based on this concept have resulted crucial for the precision measurement of rotations [7], gradients [8] and fundamental constants [9]. Differential atom interferometers have been also proposed for tests of general relativity [10], equivalence principle [11], atom neutrality [12], and for detection of gravitational waves [13]. So far, differential interferometry (DI) has been only exploited with classical resources. Its sensitivity is thus ultimately bounded by the shot noise (SN) limit, $\Delta\theta_{\rm SN} \approx 1/\sqrt{N}$, where N is the number of particles in input. For the single interferometer operation, a significant enhancement of phase sensitivity, up to the Heisenberg limit (HL) $\Delta\theta_{\rm HL} \approx 1/N$, can be obtained by using particle-entangled input states [14, 15, 16, 17]. This prediction is under intense experimental investigation with cold [18] and ultracold [19, 20, 21, 22, 23, 24] atoms. However, the analysis of a single interferometer has emphasized [25, 26, 27, 28, 29] that sub-SN cannot be reached in presence of strong phase noise. Is it possible to exploit DI with highly entangled states to overcome the SN [30] in such a noisy environment?

In this manuscript we study DI with two sensors implementing quantum resources and affected by phase noise of arbitrarily large amplitude (see Fig. 1) [31]. Our analysis takes into account the correlations of the two interferometer outcomes. It goes beyond the trivial subtraction of the two output phases estimated independently, that does not offer any significant quantum enhancement of phase sensitivity. We provides the necessary and sufficient condition, based on the Fisher information, for an entangled state to allow sub-SN phase sensitivity. We also demonstrate that the HL, which is believed to be only achievable in noiseless quantum interferometers [25, 26, 27, 28], is preserved by the lossless differential scheme as long as relative noise fluctuations are also at the HL. While the HL is saturated by maximally entangled states which are extremely fragile to particle losses, the SN can be overcome by less entangled and more robust states, as those experimentally created via particle-particle interaction in Bose-Einstein condensates (BECs) [19, 20, 21, 22, 23, 24]. These findings open the door to full exploitation of quantum resources in realistic devices, provided that a DI scheme is implemented.

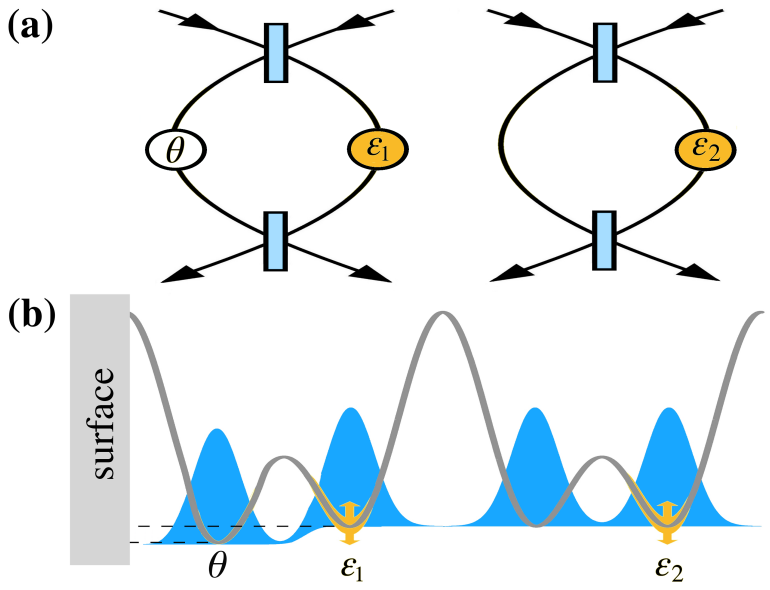

Figure 1. Differential scheme discussed in this manuscript. a) Two Mach-Zehnder interferometers affected by shot-to-shot random phase noise ϵ_1 and ϵ_2. The signal θ can be estimated in the presence of arbitrary noise, provided that relative noise fluctuations are sufficiently small. b) Application to Bose-Einstein condensates (with spatial density represented by blue filled regions) trapped in a superlattice potential (grey curve). Splitting operations in each double-well are obtained by tuning the inter-well barrier. Short range forces between atoms and a nearby surface induce a phase shift θ. Trapping potential fluctuations lead to correlations between ϵ_1 and ϵ_2.

2. Parameter estimation in differential interferometry.

Figure 1(a) shows the general DI scheme discussed in this manuscript. It consists of two interferometers running in parallel. The input state $\hat{\rho}$ is transformed by $\hat{U}(\theta,\epsilon_1,\epsilon_2) = e^{-i(\theta+\epsilon_1)\hat{J}_1} \otimes e^{-i\epsilon_2\hat{J}_2}$, where $\hat{J}_{1,2}$ are collective spin operators for the first and second interferometer, respectively. The phase shift in the first (second) interferometer is $\theta+\epsilon_1$ (ϵ_2), where θ is the "signal phase" to be estimated and $\epsilon_1,\epsilon_2 \in [-\pi,\pi]$ is the phase noise accumulated during the interferometer operations. The values of ϵ_1 and ϵ_2 change randomly in repeated shots, with probability distribution $P(\epsilon_1,\epsilon_2)$. Our general formalism does not assume a specific noise model and encompasses both Markovian and non-Markovian dephasing [we will later discuss specific forms of $P(\epsilon_1,\epsilon_2)$ and focus on the case of correlated interferometer where $\epsilon_1 = \pm\epsilon_2$]. We consider a general positive-operator value measure (POVM) $\hat{E}(\mu)$ on the output state and use an unbiased estimator $\Theta_{\rm est}(\mu_1,...,\mu_m)$, which is a function of the results obtained in m repeated independent measurements [34]. The variance of the estimator fulfills $\Delta\Theta_{\rm est} \geq \Delta\theta_{\rm CR}$ [32], where

$$\Delta\theta_{\rm CR} = \frac{1}{\sqrt{mF(\theta)}}, \tag{1}$$

is the the Cramer-Rao (CR) bound,

$$F(\theta) = \sum_{\mu} \frac{1}{P(\mu|\theta)} \left(\frac{dP(\mu|\theta)}{d\theta} \right)^2, \tag{2}$$

is the Fisher information (FI),

$$P(\mu|\theta) = \int_{-\pi}^{\pi} d\epsilon_1 \int_{-\pi}^{\pi} d\epsilon_2 \, P(\epsilon_1, \epsilon_2) P(\mu|\theta, \epsilon_1, \epsilon_2) \tag{3}$$

are conditional probabilities, and $P(\mu|\theta, \epsilon_1, \epsilon_2) = \mathrm{Tr}[\hat{E}(\mu)\hat{U}(\theta, \epsilon_1, \epsilon_2)\hat{\rho}\hat{U}^\dagger(\theta, \epsilon_1, \epsilon_2)]$. In particular, if the state $\hat{\rho}$ is separable in the two interferometers, $\hat{\rho} = \hat{\rho}_1 \otimes \hat{\rho}_2$, and the measurement in each interferometer are independent, $\hat{E}(\mu) = \hat{E}_1(\mu_1) \otimes \hat{E}_2(\mu_2)$ $[\mu \equiv (\mu_1, \mu_2)]$, then Eq. (3) becomes

$$P(\mu_1, \mu_2|\theta) = \int_{-\pi}^{\pi} d\epsilon_1 \int_{-\pi}^{\pi} d\epsilon_2 \, P(\epsilon_1, \epsilon_2) P(\mu_1|\theta + \epsilon_1) P(\mu_2|\epsilon_2). \tag{4}$$

Equation (1) takes into account the full quantum correlations of the interferometers outcomes and provides the lowest possible phase uncertainty, given the conditional probability distribution $P(\mu|\theta)$. It can be saturated for large m by the maximum-likelihood estimator [32].

3. Phase sensitivity.

Here we calculate the highest sensitivity allowed by the above DI scheme. We rewrite Eq. (3) as $P(\mu|\theta) = \mathrm{Tr}[\hat{E}(\mu)\hat{U}(\theta)\hat{\rho}_{\mathrm{eff}}\hat{U}^\dagger(\theta)]$, where $\hat{U}(\theta) \equiv e^{-i\theta\hat{J}_1} \otimes \mathbb{1}_2$ depends solely on θ and

$$\hat{\rho}_{\mathrm{eff}} \equiv \int_{-\pi}^{\pi} d\epsilon_1 d\epsilon_2 \, P(\epsilon_1, \epsilon_2) \, \hat{U}(0, \epsilon_1, \epsilon_2) \, \hat{\rho} \, \hat{U}^\dagger(0, \epsilon_1, \epsilon_2). \tag{5}$$

The noisy differential interferometer with input $\hat{\rho}$ is thus equivalent to a noiseless interferometer with effective input density matrix $\hat{\rho}_{\mathrm{eff}}$. This equivalence can be used to minimize $\Delta\theta_{\mathrm{CR}}$ over all possible POVMs [33, 34]. We have

$$\Delta\theta_{\mathrm{CR}} \geq \frac{1}{\sqrt{mF_Q[\hat{\rho}_{\mathrm{eff}}]}}, \tag{6}$$

where $F_Q[\hat{\rho}_{\mathrm{eff}}] = 4(\Delta\hat{R})^2$ is the quantum Fisher information (QFI) and $\hat{R}$ is obtained by solving $\{\hat{R}, \hat{\rho}_{\mathrm{eff}}\} = i[\hat{\rho}_{\mathrm{eff}}, \hat{J}_1 \otimes \mathbb{1}_2]$. Taking $|n_i\rangle$ the eigenbasis of $\hat{J}_i$ $[\hat{J}_i|n_i\rangle = n_i|n_i\rangle$, $-N_i/2 \leq n_i \leq N_i/2]$, where $i = 1, 2$ labels the interferometer, we have

$$\langle n_1, n_2|\hat{\rho}_{\mathrm{eff}}|m_1, m_2\rangle = C^{n_1,n_2}_{m_1,m_2} \langle n_1, n_2|\hat{\rho}|m_1, m_2\rangle, \tag{7}$$

where

$$C^{n_1,n_2}_{m_1,m_2} = \int_{-\pi}^{\pi} d\epsilon_1 d\epsilon_2 P(\epsilon_1, \epsilon_2) e^{-i[\epsilon_1(n_1 - m_1) + \epsilon_2(n_2 - m_2)]}. \tag{8}$$

Depending on $P(\epsilon_1, \epsilon_2)$, the DI may admit a decoherence free subspace (DFS) spanned by states of the system that experience no evolution under the noise [35]. For uncorrelated noise $[P(\epsilon_1, \epsilon_2) = P_1(\epsilon_1)P_2(\epsilon_2)]$ we obtain $C^{n_1,n_2}_{m_1,m_2} = 1$ if and only if $n_{1,2} = m_{1,2}$, i.e. the DFS simply reduces to the eigenstates of $\hat{J}_{1,2}$. These states are insensitive to the

phase shift and thus useless for phase estimation. As common in several differential atom interferometers, we assume that $P(\epsilon_1,\epsilon_2)=P_+(\epsilon_+)P_-(\epsilon_-)$, where $\epsilon_\pm=(\epsilon_1\pm\epsilon_2)/2$ indicates the total ("+" sign) and relative ("-" sign) noise. Equation (8) becomes

$$C^{n_1,n_2}_{m_1,m_2}=\tilde{P}_+(n_1-m_1+n_2-m_2)\tilde{P}_-(n_1-m_1-n_2+m_2), \tag{9}$$

where $\tilde{P}_\pm(k)\equiv\int_{-\pi}^{\pi}d\epsilon P_\pm(\epsilon)e^{-ik\epsilon}$. A non-trivial DFS, defined by the condition $n_1+n_2=m_1+m_2$ [$n_1-n_2=m_1-m_2$], exists in the limit of vanishing relative $P_-(\epsilon_-)=\delta(\epsilon_-)$ [total, $P_+(\epsilon_+)=\delta(\epsilon_+)$] noise fluctuations. Such DFS can be decomposed in subspaces defined by constant values of $M=n_1+n_2$ [$M=n_1-n_2$]. These, except the trivial case $M=\pm(N_1+N_2)/2$, contain coherence terms and are thus relevant for phase estimation. For vanishing total (relative) noise and in the presence of large relative (total) noise, $\hat{\rho}_{\rm eff}$ becomes block diagonal, [see Fig. 2,a] describing a statistical mixture of states with definite M values. We write $\hat{\rho}_{\rm eff}=\sum_M Q_M\hat{\rho}_M$, where $\hat{\rho}_M=\hat{\pi}_M\hat{\rho}\hat{\pi}_M$, $\hat{\pi}_M$ are projectors into the fixed-M subspace and $Q_M={\rm Tr}[\hat{\pi}_M\hat{\rho}\hat{\pi}_M]$ are weights satisfying $\sum_M Q_M=1$. We have $F_Q[\hat{\rho}_{\rm eff}]\leq\sum_M Q_M F_Q[\hat{\rho}_M]\leq 4\sum_M Q_M(\Delta\hat{J}_1)^2_M$, where $(\Delta\hat{J}_1)^2_M$ is the variance of $\hat{J}_1$ calculated for $\hat{\rho}_M$ and the second bound can be saturated by pure states. For separable states, following [16] and assuming, for simplicity, $N_1=N_2=N$, we have

$$F_Q[\hat{\rho}_{\rm eff}]\leq N-\sum_{M=\tilde{M}}^{N}(Q_M+Q_{-M})[N-(N-M)^2]\leq N, \tag{10}$$

where $\tilde{M}$ is the solution of $(N-M)^2=N$. In general,

$$F_Q[\hat{\rho}_{\rm eff}]\leq N^2-\sum_{M=1}^{N}(Q_M+Q_{-M})(2N-M)M\leq N^2. \tag{11}$$

In Eqs. (10) and (11), the QFI is maximized by populating only the $M=0$ subspace. We recover the same phase uncertainty bounds as in ideal noiseless case: the SN limit, $\Delta\theta_{\rm SN}=1/\sqrt{mN}$, for separable states, and the HL, $\Delta\theta_{\rm HL}=1/\sqrt{m}N$, for general quantum states. In other words, the condition $F_Q[\hat{\rho}_{\rm eff}]>N$, is necessary and sufficient for reaching sub-SN sensitivities. Moreover, according to Eq. (10), overcoming the SN necessarily requires particle entanglement in the effective input state. In full analogy to the noiseless case, there exist optimal entangled states providing a quadratic enhancement of phase sensitivity even in presence of large phase noise. The optimal states for DI are [in the $|m_1,m_2\rangle$ basis, see Fig. 2,b]

$$|\psi_{\rm opt}\rangle=\begin{cases}\dfrac{|N/2,-N/2\rangle+|-N/2,N/2\rangle}{\sqrt{2}} & \text{if } P_-(\epsilon_-)=\delta(\epsilon_-)\\ \dfrac{|N/2,N/2\rangle+|-N/2,-N/2\rangle}{\sqrt{2}} & \text{if } P_+(\epsilon_+)=\delta(\epsilon_+).\end{cases} \tag{12}$$

These have $F_Q=N^2$ and are not affected by phase noise. The states (12) have been experimentally realized with 2 [38] and up to 8 [39] trapped ions, and further investigated in [40]. While the saturation of the HL requires entangled interferometers, we can still have a HL scaling, i.e. $F_Q\propto N^2$ if we consider states which are separable in the two interferometers, $\hat{\rho}=\hat{\rho}_1\otimes\hat{\rho}_2$ A prominent example is the product of NOON states,

$$|\psi_{\rm NOON}\rangle=\Big(\frac{|N/2\rangle+|-N/2\rangle}{\sqrt{2}}\Big)_1\otimes\Big(\frac{|N/2\rangle+|-N/2\rangle}{\sqrt{2}}\Big)_2, \tag{13}$$

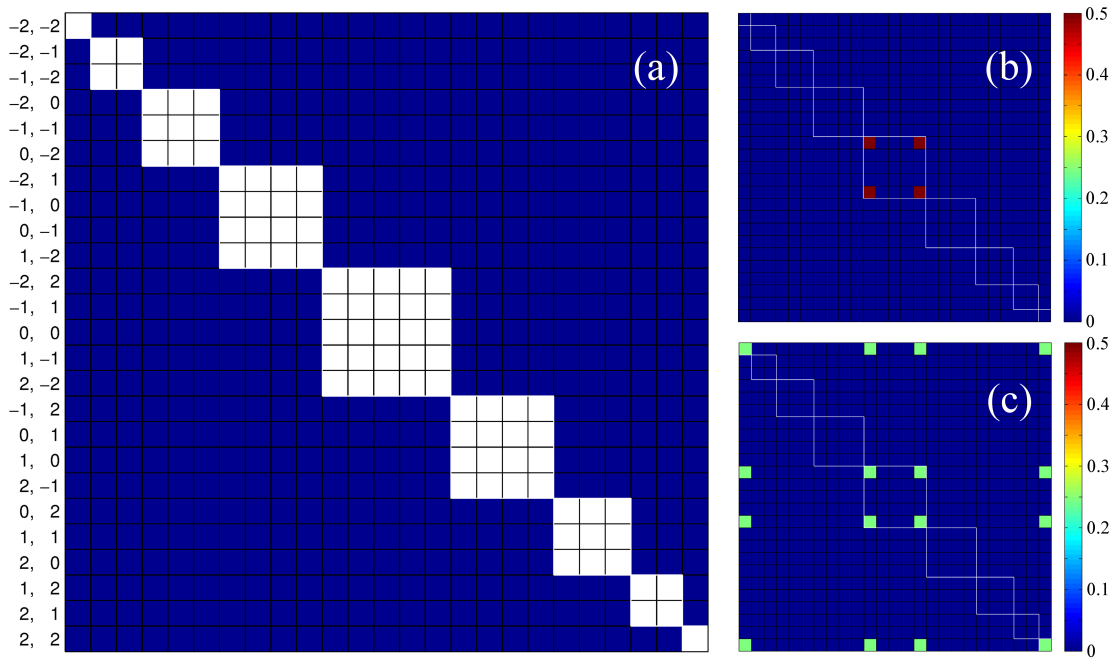

Figure 2. Panel (a) shows the general layout of a density matrix $\hat{\rho}$ of four particles in each interferometer. The basis indexes n_1, n_2 are reported on the left part of the figure. Following an opportune reordering of the basis, the DFS for vanishing relative noise fluctuations, $P_-(\epsilon_-) = \delta(\epsilon_-)$, is shown by the white squares corresponding (from top-left to bottom-right) to $M = -4, -3, -2, .., 4$. Panel (b) shows the density matrix of state (12), fully included in the central ($M = 0$) DFS. Panel (c) shows the density matrix of state (13). In the left panels the color scale is $\langle n_1, n_2|\hat{\rho}|m_1, m_2\rangle$.

which, as shown in Fig. 2,c, does not (entirely) belong to the DFS and has $F_Q = N^2/4$ both when $P_-(\epsilon_-) = \delta(\epsilon_-)$ and when $P_+(\epsilon_+) = \delta(\epsilon_+)$.

4. Differential interferometry with NOON states

In this section we study the differential interferometer scheme $\hat{U}(\theta, \epsilon_1, \epsilon_2) = (e^{-i\frac{\pi}{2}\hat{J}_x} e^{-i(\theta+\epsilon_1)\hat{J}_z})_1 \otimes (e^{-i\frac{\pi}{2}\hat{J}_x} e^{-i\epsilon_2\hat{J}_z})_2$, each interferometer being represented by the unitary transformation given by a phase shift rotation around the z axis followed by a 50-50 beam splitter. We further assume the phase noise distribution $P(\epsilon_1, \epsilon_2) = P_+(\epsilon_+)P_-(\epsilon_-)$. As input state we take the direct product of NOON states, $|\psi_{\rm NOON}\rangle_z \equiv |{\rm NOON}\rangle_{\rm z} \otimes |{\rm NOON}\rangle_{\rm z}$, with components along the z direction, $|{\rm NOON}\rangle_z = (|N/2\rangle_z + |-N/2\rangle_z)/\sqrt{2}$ [41], $|\mu\rangle_z$ being an eigenstate of $\hat{J}_z$ with eigenvalue μ. In the following we provide the conditional probabilities and FI when $P_\pm(\epsilon_\pm)$ are even functions of $\epsilon_\pm$ and specialize to the case a Gaussian noise distributions. For a discussion on more general noise functions see Appendix C.

The probability to measure a relative number of particles μ_1 at the output of the interferometer 1 and μ_2 at the output of interferometer 2 can be calculated analytically

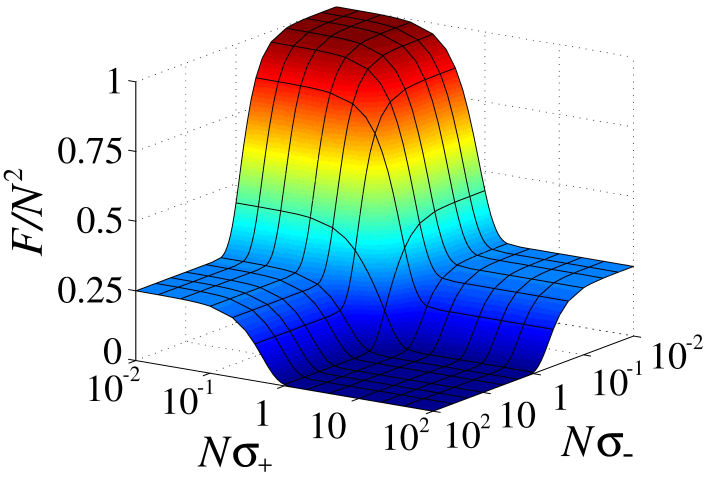

Figure 3. Fisher information (maximized over θ) for a differential interferometer with noise distribution given by Eq. (17) and factorized NOON states Eq. (13) as input (see text for details). Here $N = 100$.

and is given by (see Appendix C for details on the derivation of the equations below)

$$P(\mu_1,\mu_2|\theta) = \left(\frac{N!}{2^N}\right)^2 \frac{1}{(\frac{N}{2}-\mu_1)!(\frac{N}{2}+\mu_1)!(\frac{N}{2}-\mu_2)!(\frac{N}{2}+\mu_2)!} \times \\ \times \left[1+(-1)^{\mu_2}V_N^+V_N^- + (-1)^{\mu_1}\left(V_N^+V_N^- + \frac{(-1)^{\mu_2}}{2}(V_{2N}^+ + V_{2N}^-)\right)\cos N\theta\right], \tag{14}$$

where $V_K^\pm \equiv \int_{-\pi}^{\pi} d\epsilon_\pm P_\pm(\epsilon_\pm)\cos(K\epsilon_\pm)$. The FI is

$$F(\theta) = \frac{N^2\sin^2 N\theta}{2}\left[\frac{A_-B_-^2}{A_-^2 - B_-^2\cos^2 N\theta} + \frac{A_+B_+^2}{A_+^2 - B_+^2\cos^2 N\theta}\right], \tag{15}$$

where $A_\pm(N) \equiv 1 \pm V_N^+V_N^-$, $B_\pm(N) \equiv V_N^+V_N^- \pm (V_{2N}^+ + V_{2N}^-)/2$. The optimal value of the FI, $F \equiv \max_\theta F(\theta)$, is reached for $\cos N\theta = 0$,

$$F = \frac{N^2}{2}\left[\frac{B_-^2(N)}{A_-(N)} + \frac{B_+^2(N)}{A_+(N)}\right]. \tag{16}$$

Let us discuss the different limit values of Eq. (16) taking into account that $V_K^\pm = 1$ when $P_\pm(\epsilon_\pm) = \delta(\epsilon_\pm)$ and $V_K^\pm = 0$ when $P_\pm(\epsilon_\pm) = 1/2\pi$. If relative noise fluctuations are vanishingly small, $P_-(\epsilon_-) = \delta(\epsilon_-)$, Eq. (16) ranges from $F = N^2$ [if also $P_+(\epsilon_+) = \delta(\epsilon_+)$, corresponding to the ideal noiseless limit] to $F = N^2/4$ [when $P_+(\epsilon_+) = 1/2\pi$]. In other words, if the relative noise between the two interferometers is fixed, a phase sensitivity at the HL can be obtained for arbitrary large total noise (i.e. arbitrary large noise in *each* interferometer). If total noise fluctuations are large, $P_+(\epsilon_+) = 1/2\pi$, we obtain $F = N^2(V_{2N}^-)^2$, which predicts the HL for $V_{2N}^- \approx 1$ and sub-SN for $V_{2N}^- > 1/\sqrt{N}$. In Fig. 3(c) we plot Eq. (16) as a function of $\sigma_\pm$ taking

$$P(\epsilon_\pm) = \frac{e^{(\cos\epsilon_\pm)/\sigma_\pm^2}}{2\pi I_0(1/\sigma_\pm^2)}, \tag{17}$$

where $I_0(x)$ is the modified Bessel function of the first kind. This noise function continuously interpolates from a Gaussian distribution of width $\sigma_\pm$, when $\sigma_\pm \ll 1$, to a flat distribution, when $\sigma_\pm \gg 1$. The condition $V_{2N}^- \approx 1$ is thus equivalent to $\sigma_- \approx 1/N$, while $V_{2N}^- \gtrsim 1/\sqrt{N}$ is recovered for $\sigma_- \lesssim \sqrt{\log N}/N$. These results show that reaching the HL in the differential interferometer requires relative noise fluctuations at the HL itself.

5. Precision limit for DI with Bose-Einstein condensates.

In this section we discuss a differential Mach-Zehnder (MZ) interferometer $\hat{U}(\theta, \varepsilon_1, \varepsilon_2) = (e^{-i(\theta+\varepsilon_1)\hat{J}_y})_1 \otimes (e^{-i\varepsilon_2\hat{J}_y})_2$ with input states that can be created with two-mode BECs. We consider phase estimation from the measurement of the number of particles in output. We further take vanishing relative phase noise fluctuations in the two interferometers, $P_-(\epsilon_-) = \delta(\epsilon_-)$, and $P(\epsilon_+)$ given by Eq. (17).

We first consider adiabatic state preparation [42], focusing on the ground state $|\psi_{\rm gs}(\Lambda)\rangle$ of the Hamiltonian $\hat{H} = \hbar\chi\hat{J}_z^2 - \hbar\Omega\hat{J}_x$, with $\Lambda \equiv N\chi/\Omega$. This can be implemented in a double-well trap [see Fig. 1(b)] with χ and Ω interaction and tunneling parameters, respectively [19, 22]. We can distinguish Rabi, $0 < \Lambda \leq 1$, Josephson, $1 < \Lambda \leq N^2$, and Fock, $\Lambda > N^2$, regimes. In the ideal case, these regimes are characterized by different scalings of the FI (optimized in θ): $F \sim N$ ($F = N$ for the spin coherent state, $|N/2\rangle_x$, $\Lambda = 0$), $F \sim N^{3/4}$, and $F \sim N^2$ [$F = N^2/2 + N$ [43] for the twin-Fock state, $|0\rangle_z$, $\Lambda = \infty$], respectively [44]. In Fig. 4(a) we report the FI as a function of Λ for the differential MZ with input $|\psi_{\rm gs}(\Lambda)\rangle \otimes |\psi_{\rm gs}(\Lambda)\rangle$. Different lines refer to different value of $N \times \sigma_+$, ranging from the noiseless case ($\sigma_+ = 0$, thick dashed line) to uniform phase noise ($\sigma_+ = \infty$, thick solid line). The twin-Fock is optimal for $\sigma_+ \lesssim 1/N$, while for $\sigma_+ \to \infty$ the FI is maximized at $\Lambda \approx N$.

We further consider states that are created by the nonlinear evolution $|\psi_{\rm dyn}(\tau)\rangle = e^{i\delta\hat{J}_n}\, e^{-i\hat{J}_z^2\tau}|N/2\rangle_x$ starting from a spin coherent state [20, 14, 45], where $\tau = \chi t$. Here $e^{i\delta\hat{J}_n}$ rotates the state so to maximize the FI in the noiseless case [16, 46]. In Fig 4(b) we show the FI for the differential MZ with input $|\psi_{\rm dyn}(\tau)\rangle \otimes |\psi_{\rm dyn}(\tau)\rangle$. Lines are as in Fig. 4(a). Interestingly, the short time dynamics ($\tau \lesssim 1/\sqrt{N}$, where spin squeezing is created [45]) is robust and sub-SN is found also for large phase noise. The characteristic plateau ($F = N^2/2$ for the ideal case [16]) is washed out when $\sigma_+ \gtrsim 1/N$. The FI at large values of σ_+ is characterized by several peaks, the most prominent found in correspondence to the creation of macroscopic superposition states ("phase cats") with multiple (larger than two) components. The long-time dynamics at $\tau = \pi/2$ leads to maximally entangled states (a two components phase cat) having $F = N^2/4$, as discussed above.

For specific input states, we have repeated the previous analysis for large values of N (up to $N \approx 1000$) and $\sigma_+ = \infty$ (flat total noise case). The results are shown in Fig. 4(c). The FI reaches an asymptotic power law scaling $F = \beta N^\alpha$: $\beta = 0.5$, $\alpha = 1$ for coherent spin state (green diamonds); $\beta = 0.2$, $\alpha = 1.5$ for the optimal states of

the adiabatic preparation at $\Lambda \approx N$ (red squares); $\beta = 0.3$, $\alpha = 1.4$ for the optimal states of the diabatic preparation at time $\tau \approx 1/N^{3/4}$ (blue circles); $\beta = 0.39, \alpha = 1.17$ for the twin-Fock state (black dots). The solid black line is the analytical NOON state result ($\alpha = 2$, $\beta = 1/4$) discussed previously. The twin-Fock state is an interesting and experimentally relevant [21] example. It is strongly entangled and reaches a HL scaling in the single noiseless MZ, however it performs only slightly better than the SN in the differential MZ with large noise and large number of particles. In Fig 4(d) we further investigated the FI for the twin-Fock state as a function of N, for different values of σ_+ (dots). For $N \lesssim 1/\sigma_+$ and $\sigma_+ \ll 1$, the FI follows the ideal behavior $F = N^2/2 + N$ (dashed line). For $N \gg 1/\sigma_+$, we recover roughly the same scaling of FI ($F \propto N^{1.17}$) as in the large phase noise case.

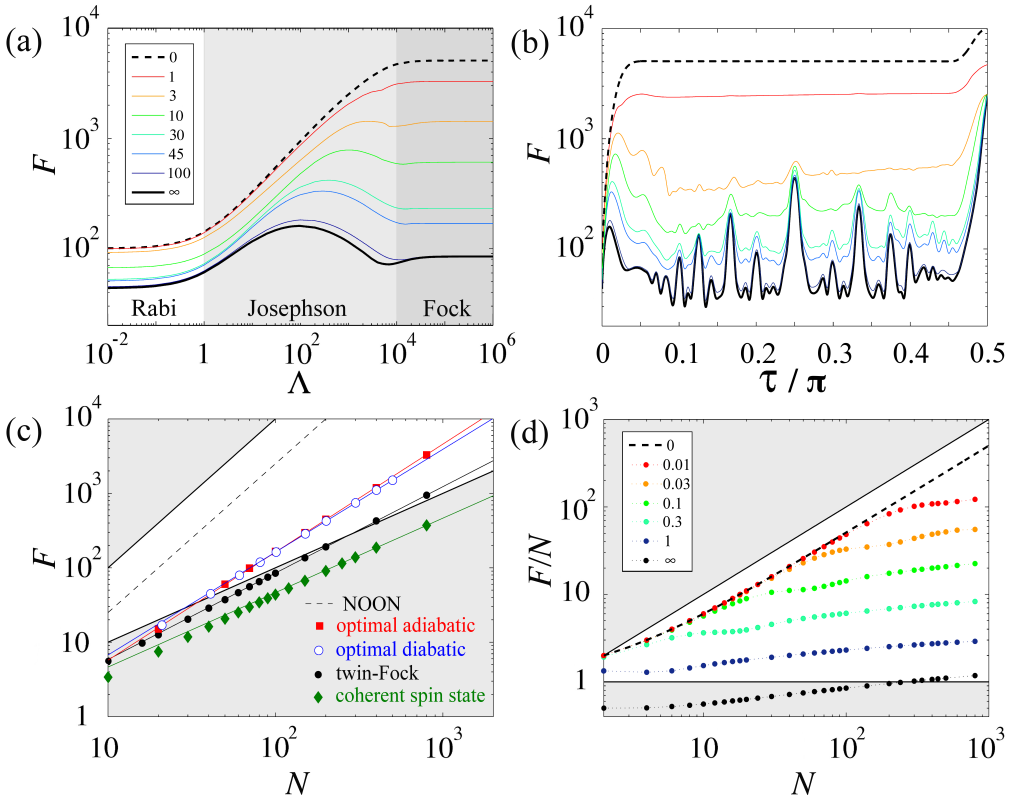

Figure 4. a) FI as a function of Λ for the adiabatic state preparation. The shadow regions highlight different regimes (see text). b) FI as a function of τ for the diabatic state preparation. In panels (a) and (b) $N = 100$ and different lines refer to different values of $N \times \sigma_+$. c) FI as a function of N for various input states of the differential MZ interferometer for $\sigma_+ = \infty$. Solid thin lines are fits while solid thick lines are the HL and SN (the white region between the two lines corresponds to sub-SN). d) FI for the twin-Fock state as a function of N and for different σ_+ values. Think lines and colored regions are as in panel (c).

6. Conclusions.

In this manuscript we have extended the analysis of DI to the domain of entangled states. It is not obvious, a priori, that DI can suppresses spurious phase noise when highly entangled – and thus extremely fragile against phase noise fluctuations – states are used. Our analysis reveals that when the phase noise is perfectly correlated in the two interferometers, and losses can be neglected, there exists a decoherence free subspace where entanglement is passively protected. We have thus identified a class of entangled input state that can provide a sub-SN sensitivity in a differential interferometer up to the HL, even for large noise. This class is non trivial, fully characterized by the FI, and includes states that have been recently created experimentally. We expect our results to be a guideline for quantum-enhanced realistic interferometers in the near future.

7. Acknowledgment.

This work has been supported by the EU-STREP Project QIBEC and ERC StG No. 258325. L.P. and M.F. acknowledge financial support by MIUR through FIRB Project No. RBFR08H058.

Appendix A. Derivation of Eq. (3).

We here derive Eq. (3) from first principles. We start from the joint probability density $P(\mu,\theta,\epsilon_1,\epsilon_2)$ and integrate over ϵ_1 and ϵ_2,

$$P(\mu,\theta)=\int_{-\pi}^{\pi} d\epsilon_1 d\epsilon_2\, P(\mu,\theta,\epsilon_1,\epsilon_2) \tag{A.1}$$

so to eliminate nuisance parameters. By using the relation $P(x,y)=P(x|y)P(y)$ between joint and conditional probabilities, where x and y are random variables, we have

$$P(\mu|\theta)=\frac{P(\mu,\theta)}{P(\theta)}=\int_{-\pi}^{\pi} d\epsilon_1 d\epsilon_2\, P(\mu|\theta,\epsilon_1,\epsilon_2)P(\epsilon_1,\epsilon_2|\theta). \tag{A.2}$$

Since $\epsilon_{1,2}$ do not depend on θ, i.e. $P(\epsilon_1,\epsilon_2|\theta)=P(\epsilon_1,\epsilon_2)$, we recover Eq. (3).

Appendix B. Derivation of inequalities (10) and (11).

Here we detail the calculation of $4\sum_M Q_M(\Delta\hat{J}_1)^2_M$, where $(\Delta\hat{J}_1)^2_M$ is the variance of the operator $\hat{J}_1$ calculated on the fixed-M subspace. We consider the case $N_1=N_2=N/2$ for simplicity. We have $4(\Delta\hat{J}_1)^2_M\leq(\max_M n_1-\min_M n_1)^2$, where $-N/2\leq n_1\leq N/2$ are the eigenvalues of $\hat{J}_1$ and $\max_M n_1$ ($\min_M n_1$) are the maximum (minimum) values of n_1 in the fixed-M DFS. In general, $\max_M n_1=\min(M+N/2,N/2)$ and $\min_M n_1=\max(M-N/2,-N/2)$. We thus have

$$4(\Delta\hat{J}_1)^2_M\leq(N-|M|)^2, \tag{B.1}$$

with equality of ρ_M is the equal-weighted superposition of states with the maximum and the minimum value of n_1 in the fixed-M DFS. Taking into account that $\sum_{M=-N}^{N} Q_M = 1$

$$\begin{aligned} 4\sum_M Q_M(\Delta\hat{J}_1)^2_M &= Q_0 N^2 + \sum_{M=1}^{N}(Q_M + Q_{-M})(N-M)^2 \\ &= N^2 - \sum_{M=1}^{N}(Q_M + Q_{-M})M(2N-M) \end{aligned}$$

We thus recover Eq. (11). Since $M \leq 2N$, the second term in the equation above is nonnegative and we find $4\sum_M Q_M(\Delta\hat{J}_1)^2_M \leq N^2$. For separable states, we need to further take into account that $4(\Delta\hat{J}_1)^2_M \leq N$ [16]. We thus have

$$4(\Delta\hat{J}_1)^2_M \leq \min\left[(N-|M|)^2, N\right], \tag{B.2}$$

and thus obtain

$$\begin{aligned} 4\sum_M Q_M(\Delta\hat{J}_1)^2_M &= Q_0 N + \sum_{M=1}^{N}(Q_M + Q_{-M})\min\left[(N-M)^2, N\right] \\ &= Q_0 N - \sum_{M=\tilde{M}}^{N}(Q_M + Q_{-M})[N-(N-M)^2], \end{aligned}$$

which follows since for $\tilde{M} \leq M \leq N$ we have $\min[N,(N-M)^2] = (N-M)^2$. We recover Eq. (10). Since for $\tilde{M} \leq M \leq N$ we have $N-(N-M)^2 \geq 0$, the second term in the above equation is nonnegative and we have $4\sum_M Q_M(\Delta\hat{J}_1)^2_M \leq N$ for separable states.

Appendix C. Extension of the discussion of Sec. 4 to arbitrary noise distributions.

Here we provide a detailed derivation of the equations presented in Sec. 4 and extend the discussion to arbitrary noise distributions. Let us first calculate the conditional probability distribution of the relative number of particles for the single interferometer with a NOON probe state:

$$\begin{aligned} P(\mu|\phi) &= |{}_z\langle\mu|e^{-i\frac{\pi}{2}\hat{J}_x}e^{-i\phi\hat{J}_z}|\mathrm{NOON}\rangle_z|^2 \\ &= \left|\frac{{}_z\langle\mu|e^{-i\frac{\pi}{2}\hat{J}_x}|+N/2\rangle_z + e^{i\phi N}{}_z\langle\mu|e^{-i\frac{\pi}{2}\hat{J}_x}|-N/2\rangle_z}{\sqrt{2}}\right|^2. \end{aligned}$$

The rotation matrix elements ${}_z\langle\mu|e^{-i\frac{\pi}{2}\hat{J}_x}|\pm N/2\rangle_z$ are given by

$$\begin{aligned} {}_z\langle\mu|e^{-i\frac{\pi}{2}\hat{J}_x}|+N/2\rangle_z &= \frac{e^{-i\frac{\pi}{2}(\mu-\frac{N}{2})}}{2^{N/2}}\sqrt{\frac{N!}{(N/2-\mu)!(N/2+\mu)!}}, \\ {}_z\langle\mu|e^{-i\frac{\pi}{2}\hat{J}_x}|-N/2\rangle_z &= \frac{e^{-i\frac{\pi}{2}(\mu+\frac{N}{2})}}{2^{N/2}}\sqrt{\frac{N!}{(N/2+\mu)!(N/2+\mu)!}}(-1)^{\frac{N}{2}+\mu}. \end{aligned}$$

We thus obtain

$$P(\mu|\theta) = \frac{1}{2^N}\frac{N!}{(N/2-\mu)!(N/2+\mu)!}\left|\frac{e^{-i\frac{N}{2}\phi} + (-1)^\mu e^{i\frac{N}{2}\phi}}{\sqrt{2}}\right|^2, \tag{C.1}$$

with

$$\left|\frac{e^{-i\frac{N}{2}\phi}+(-1)^{\mu}e^{i\frac{N}{2}\theta}}{\sqrt{2}}\right|^2=\begin{cases}1+(-1)^{\mu}\cos N\phi & \text{if } N \text{ is even},\\ 1+(-1)^{\mu+1/2}\sin N\phi & \text{if } N \text{ is odd}.\end{cases}$$

We now consider the differential sensor described by the unitary operator $\hat{U}(\theta,\epsilon_1,\epsilon_2)=(e^{-i\frac{\pi}{2}\hat{J}_x}e^{-i(\theta+\epsilon_1)\hat{J}_z})_1\otimes(e^{-i\frac{\pi}{2}\hat{J}_x}e^{-i\epsilon_2\hat{J}_z})_2$, each interferometer being given by the transformation $(e^{-i\frac{\pi}{2}\hat{J}_x}e^{-i(\phi_i)\hat{J}_z})_i$, $i=1,2$. We take a NOON state of N particles as input of each interferometer (without loss of generality we assume N to be even) and estimate the phase shift from the measurement of the relative number of particles at the output ports of each interferometer, $\hat{E}(\mu)\equiv\hat{E}(\mu_1,\mu_2)=(|\mu_1\rangle_z\langle\mu_1|)_1\otimes(|\mu_2\rangle_z\langle\mu_2|)_2$. Taking $P(\epsilon_1,\epsilon_2)=P_+(\epsilon_+)P_-(\epsilon_-)$, where $\epsilon_\pm=(\epsilon_1\pm\epsilon_2)/2$, Eq. (4) writes

$$P(\mu_1,\mu_2|\theta)=\int_{-\pi}^{\pi}d\epsilon_+P_+(\epsilon_+)\int_{-\pi}^{\pi}d\epsilon_-P_-(\epsilon_-)P(\mu_1|\theta+\epsilon_++\epsilon_-)P(\mu_2|\epsilon_+-\epsilon_-),$$

with $P(\mu_i|\phi_i)$ $(i=1,2)$ given by Eq. (C.1). After straightforward algebra we obtain

$$P(\mu_1,\mu_2|\theta)=\Big(\frac{N!}{2^N}\Big)^2\frac{\mathcal{A}_N(\mu_2)+\mathcal{C}_N(\mu_1,\mu_2)\cos N\theta-\mathcal{S}_N(\mu_1,\mu_2)\sin N\theta}{(\frac{N}{2}-\mu_1)!(\frac{N}{2}+\mu_1)!(\frac{N}{2}-\mu_2)!(\frac{N}{2}+\mu_2)!},$$

where

$$\begin{aligned}\mathcal{A}_N(\mu_2)&=1+(-1)^{\mu_2}[V_N^+V_N^-+W_N^+W_N^-],\\ \mathcal{C}_N(\mu_1,\mu_2)&=(-1)^{\mu_1}\Big[V_N^+V_N^--W_N^+W_N^-\Big]+(-1)^{\mu_1+\mu_2}\Big(\frac{V_{2N}^++V_{2N}^-}{2}\Big),\\ \mathcal{S}_N(\mu_1,\mu_2)&=(-1)^{\mu_1}\Big[V_N^+W_N^-+W_N^+V_N^-\Big]+(-1)^{\mu_1+\mu_2}\Big(\frac{W_{2N}^++W_{2N}^-}{2}\Big),\end{aligned}\tag{C.2}$$

and

$$V_K^{\pm}\equiv\int_{-\pi}^{\pi}d\epsilon_\pm P_\pm(\epsilon_\pm)\cos(K\epsilon_\pm),\quad W_K^{\pm}\equiv\int_{-\pi}^{\pi}d\epsilon_\pm P_\pm(\epsilon_\pm)\sin(K\epsilon_\pm),\tag{C.3}$$

K being an integer number. We are now ready to compute the FI, Eq. (2),

$$F(\theta)=\sum_{\mu_1,\mu_2=-N/2}^{N/2}\frac{1}{P(\mu_1,\mu_2|\theta)}\Big(\frac{dP(\mu_1,\mu_2|\theta)}{d\theta}\Big)^2.$$

The FI can be written as the sum of three terms:

$$F(\theta)=N^2[\mathcal{F}_C(N,\theta)\cos^2N\theta+\mathcal{F}_{SC}(N,\theta)\sin 2N\theta+\mathcal{F}_S(N,\theta)\sin^2N\theta],\tag{C.4}$$

where the coefficients $\mathcal{F}_C(N,\theta)$, $\mathcal{F}_S(N,\theta)$ and $\mathcal{F}_{SC}(N,\theta)$ are function of N and $N\theta$ and are gives by a sums over μ_1 and μ_2. To compute the sums we separate the sum over $\mu_{1,2}$ into sum over odd $\mu_{1,2}$ and sum over even $\mu_{1,2}$ (since N is assumed to be even, μ_1 and μ_2 are integer numbers) and take into account that

$$\sum_{\mu,\text{odd}}\frac{1}{2^N}\frac{N!}{(N/2-\mu)!(N/2+\mu)!}=\sum_{\mu,\text{even}}\frac{1}{2^N}\frac{N!}{(N/2-\mu)!(N/2+\mu)!}=\frac{1}{2}.$$

We thus obtain

$$\mathcal{F}_C(N,\theta) = \frac{1}{2}\frac{\mathcal{S}_N^2(0,1)\mathcal{A}_N(1)}{\mathcal{A}_N^2(1) - [\mathcal{C}_N(0,1)\cos N\theta - \mathcal{S}_N(0,1)\sin N\theta]^2} + \\ + \frac{1}{2}\frac{\mathcal{S}_N^2(0,0)\mathcal{A}_N(0)}{\mathcal{A}_N^2(0) - [\mathcal{C}_N(0,0)\cos N\theta - \mathcal{S}_N(0,0)\sin N\theta]^2},$$

$$\mathcal{F}_S(N,\theta) = \frac{1}{2}\frac{\mathcal{C}_N^2(0,1)\mathcal{A}_N(1)}{\mathcal{A}_N^2(1) - [\mathcal{C}_N(0,1)\cos N\theta - \mathcal{S}_N(0,1)\sin N\theta]^2} + \\ + \frac{1}{2}\frac{\mathcal{C}_N^2(0,0)\mathcal{A}_N(0)}{\mathcal{A}_N^2(0) - [\mathcal{C}_N(0,0)\cos N\theta - \mathcal{S}_N(0,0)\sin N\theta]^2},$$

and

$$\mathcal{F}_{SC}(N,\theta) = \frac{1}{2}\frac{\mathcal{C}_N(0,1)\mathcal{S}_N(0,1)\mathcal{A}_N(1)}{\mathcal{A}_N^2(1) - [\mathcal{C}_N(0,1)\cos N\theta - \mathcal{S}_N(0,1)\sin N\theta]^2} + \\ + \frac{1}{2}\frac{\mathcal{C}_N(0,0)\mathcal{S}_N(0,0)\mathcal{A}_N(0)}{\mathcal{A}_N^2(0) - [\mathcal{C}_N(0,0)\cos N\theta - \mathcal{S}_N(0,0)\sin N\theta]^2}.$$

The above equations allow to calculate the FI given an arbitrary relative and total noise functions. For the case of NOON input states considered here, the FI ultimately depends on the eight Fourier coefficients $V_N^{\pm}$, $V_{2N}^{\pm}$, $W_N^{\pm}$ and $W_{2N}^{\pm}$. Below, we first shown how the calculation of the FI simplifies when noise distributions are even functions of $\varepsilon_{\pm}$. Furthermore, we study the case of perfectly correlated relative noise and arbitrary total noise distribution.

Symmetric noise distributions. If $P_{\pm}(\epsilon_{\pm})$ are even functions of $\epsilon_{\pm}$, the calculation of the Fsiher information simplify notably. We have $W_K^{\pm} = 0$, which implies $\mathcal{S}_N(\mu_1,\mu_2) = 0$ for all μ_1 and μ_2, $\mathcal{F}_C(N,\theta) = 0$ and $\mathcal{F}_{SC}(N,\theta) = 0$. We also have $\mathcal{A}_N^2(0) = 1 + V_N^+ V_N^- = A_+$, $\mathcal{A}_N^2(1) = 1 - V_N^+ V_N^- = A_-$, $\mathcal{C}_N(0,1) = V_N^+ V_N^- - (V_{2N}^+ + V_{2N}^-)/2 = B_-$ and $\mathcal{C}_N(0,0) = V_N^+ V_N^- + (V_{2N}^+ + V_{2N}^-)/2 = B_+$, where $A_{\pm}$ and $B_{\pm}$ have been introduced in Sec. 4. The conditional probability and the FI reduce to Eqs. (14) and (15), respectively.

Perfectly correlated relative noise. In the following we consider the ideal case of perfectly correlated relative noise, $P_-(\varepsilon_-) = \delta(\varepsilon_-)$. This implies $V_N^- = V_{2N}^- = 1$, $W_N^- = W_{2N}^- = 0$ and Eqs. (C.2) simplify to

$$\begin{aligned}
\mathcal{A}_N(\mu_2) &= 1 + (-1)^{\mu_2} V_N^+, \\
\mathcal{C}_N(\mu_1,\mu_2) &= (-1)^{\mu_1} V_N^+ + (-1)^{\mu_1+\mu_2}\Big(\frac{1+V_{2N}^+}{2}\Big), \\
\mathcal{S}_N(\mu_1,\mu_2) &= (-1)^{\mu_1} W_N^+ + (-1)^{\mu_1+\mu_2}\frac{W_{2N}^+}{2}.
\end{aligned}$$

These equation are the basis of further considerations. For instance, if $P_+(\varepsilon)$ [we indicate $\varepsilon \equiv \varepsilon_+$ to simplify the notation] is an odd function of ε plus a constant providing normalization in the 2π interval, then $V_K^+ = 0$ and we can expand it in Fourier series as

$$P_+(\varepsilon) = \frac{1}{2\pi} + \frac{1}{\pi}\sum_{K=1}^{+\infty} W_K^+ \sin K\varepsilon.$$

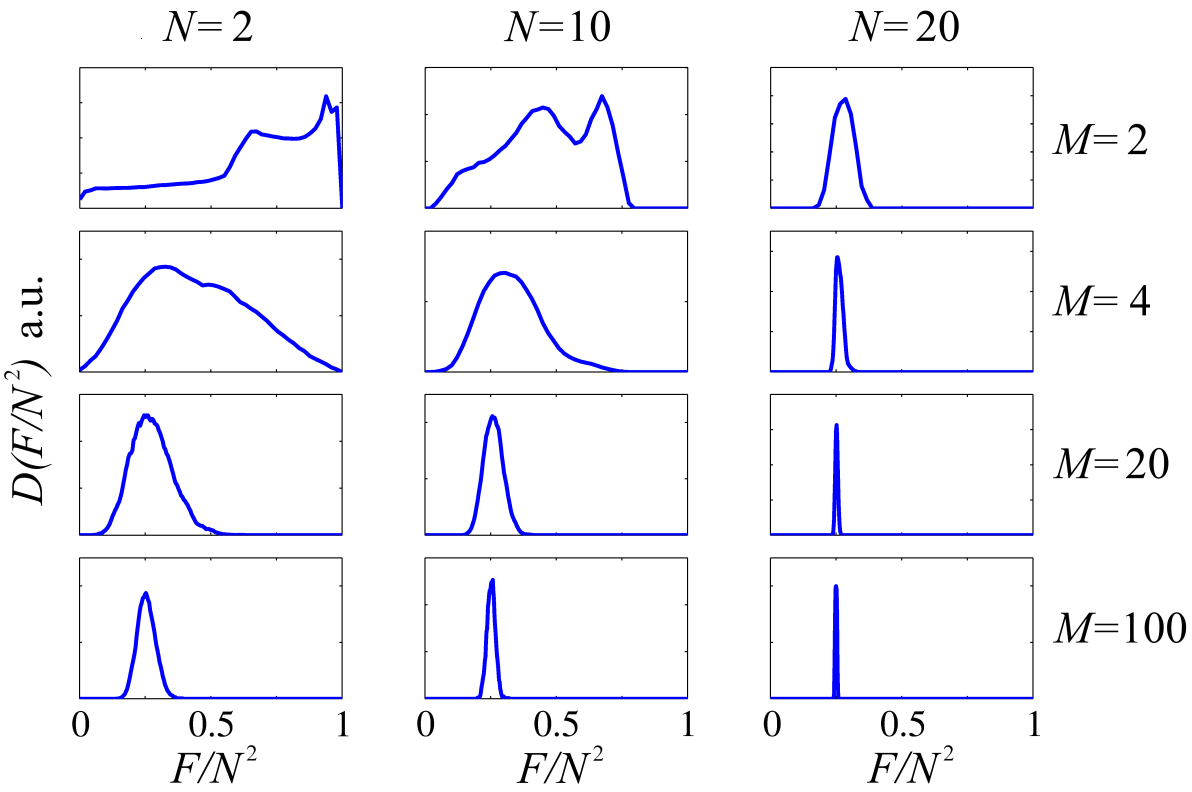

Figure C1. Statistical distribution of the F/N^2, $D(F/N^2)$, obtained by taking Eq. (C.5) as (total) phase noise distribution. The different panels refer to different number of particles, N, (different columns) and number, M, of noise peaks in Eq. (C.5) (different rows). Here $\sigma = 2\pi/100$.

The condition $P_+(\varepsilon) \geq 0$ implies $4\pi^2|\sum_{K=1}^{+\infty} W_K^+ \sin K\varepsilon|^2 \leq 1$ which, integrating over ε gives $\sum_{K=1}^{+\infty}(W_K^+)^2 \leq 1/2$. In this case, evaluating $F(\theta)$ at phase values θ such that $\cos N\theta = 0$, we have [we recall that $F \equiv \max_\theta F(\theta)$]

$$\frac{F}{N^2} \geq \frac{1}{8}\left(\frac{1}{1-(W_N^+ - W_{2N}^+/2)^2} + \frac{1}{1-(W_N^+ + W_{2N}^+/2)^2}\right).$$

The term between brackets does not diverge because of the condition $\sum_{K=1}^{+\infty}(W_K^+)^2 \leq 1/2$ and it is always larger than two. It implies that, in this case $F \geq N^2/4$. To treat a more general case, we consider the noise distribution

$$P_+(\varepsilon) \propto \sum_{n=1}^{M} e^{\cos(\epsilon - x_n)/\sigma^2} \tag{C.5}$$

which is a normalized sum of M peaks of width σ (for $\sigma \ll 1$ $e^{\cos(\epsilon-x_n)/\sigma^2} \approx e^{-(\epsilon-x_n)^2/2\sigma^2}$, the cos function being used to take into account the 2π-periodicity) centered at random positions $x_1, x_2, ..., x_M \in [-\pi, \pi]$. For random choices of $x_1, x_2, ..., x_M$ we calculate the FI and maximize over θ. In Fig. (C1) we plot the statistical distribution of $F = \max_\theta F(\theta)$ as a function of N and M.

For sufficiently large values of N and/or M, the noise distribution (C.5) has vanishing high frequency Fourier components. When increasing M (at fixed value of N and σ) this is due to the fact that the noise distribution tends to become flat in most of the random realizations (i.e. for most of the random choices of $x_1, x_2, ..., x_M$). When increasing N (at fixed σ and σ), this is due to the vanishing tails in the Fourier spectrum of $e^{\cos(\epsilon - x_n)/\sigma^2}$. In both cases, the coefficients V_N^+, W_N^+, V_{2N}^+ and W_{2N}^- are vanishing small, and we have

$$\mathcal{A}_N(\mu_2) = 1, \qquad \mathcal{C}_N(\mu_1, \mu_2) = \frac{(-1)^{\mu_1+\mu_2}}{2}, \qquad \mathcal{S}_N(\mu_1, \mu_2) = 0,$$

and

$$F(\theta) = \frac{N^2 \sin^2 N\theta}{4 - \cos^2 N\theta}, \tag{C.6}$$

giving $F \equiv \max_\theta F(\theta) = N^2/4$. In Fig. C1 we indeed observe that the distribution of F peaks around $1/4$ for sufficiently large values of N and M.

For small values of M and N we may have a situations where F/N^2 is very small. In general, for a fixed number of particles, it is possible to derive pathologic noise distributions for which the FI vanishes. To see this, it is convenient to rewrite $F(\theta)$ as

$$\frac{F(\theta)}{N^2} = \frac{(1 - V_N^+)U_1^2(\theta)}{2D_1(\theta)} + \frac{(1 + V_N^+)U_0^2(\theta)}{2D_0(\theta)}, \tag{C.7}$$

with

$$U_j(\theta) = \left(W_N^+ + (-1)^j \frac{W_{2N}^+}{2}\right) \cos N\theta + \left(V_N^+ + (-1)^j \frac{1 + V_{2N}^+}{2}\right) \sin N\theta,$$

and

$$D_j(\theta) = \left(1 + (-1)^j V_N^+\right)^2 - \left[\left(V_N^+ + (-1)^j \frac{1 + V_{2N}^+}{2}\right) \cos N\theta - \right.$$
$$\left. - \left(W_N^+ + (-1)^j \frac{W_{2N}^+}{2}\right) \sin N\theta\right]^2,$$

with $j = 0, 1$. It's possible to demonstrate that $D_{1,0} > 0 \ \forall\theta$. Therefore the Fisher is zero only if both numerators are zero. It is also possible to see that the cases involving $V_N^+ = \pm 1$ and $U_{0,1} = 0$ lead to non-physical probability distributions. The only remaining option is to have both $U_{0,1}(\theta) = 0 \ \forall\theta$. This in turn corresponds to a probability distribution with $V_N^+ = 0$, $W_N^+ = 0$, $W_{2N}^+ = 0$ and $V_{2N}^+ = -1$. Recalling the definition of V_{2N}^+, we thus have that $F(\theta) = 0$ is and only if

$$\int d\epsilon \, P(\epsilon) \cos^2 N\epsilon = 0. \tag{C.8}$$

This integral involves two positive functions. Equation (C.8) is thus fulfilled only if P_+ to have support in correspondence to the zeroes of $\cos N\epsilon$. A total noise distribution $P(\epsilon)$ for which the FI vanishes is therefore obtained as a normalized sum of Dirac deltas symmetrically centered at the zeroes of $\cos N\epsilon$. We argue that this situation is pathological for NOON states where the FI is entirely determined by the Fourier components of $P(\varepsilon)$, Eq. (C.3), at $K = N$ and $K = 2N$. Furthermore, if $P(\epsilon)$, instead of being a sum of Dirac peaks, is a sum of peaks of finite width, we recover, as noticed above, Eq. (C.6) for N sufficiently large.

Appendix D. Numerical Method to compute the Fisher Information

Here we report a method for the numerical calculation of the FI that we used to obtain the results of Sec. 5. Here we consider a differential interferometer and indicate with μ_1 and μ_2 the results of a measurement at the outputs of the two devices. The differential interferometer transformation is $\hat{U}(\theta, \varepsilon_1, \varepsilon_2) = e^{-i(\theta+\varepsilon_1)\hat{J}_1} \otimes e^{-i\varepsilon_2\hat{J}_2}$ and the joint conditional probability reads

$$P(\mu_1, \mu_2|\theta) = \int_{-\pi}^{\pi} d\epsilon\, P(\mu_1|\theta+\epsilon)P(\mu_2|\epsilon)P(\epsilon), \tag{D.1}$$

where we have assumed $P_-(\epsilon_-) = \delta(\epsilon_-)$. Noticing that the functions $P(\mu_i|x)$, $i = 1, 2$, are 2π periodic in x, it is therefore possible to make a Fourier expansion of the functions. This is conveniently done with a Fast Fourier Transform algorithm. Furthermore, the discretized atom number poses a maximum allowed frequency in the decomposition given by Shannon's criterion:

$$P(\mu_i|x) = \frac{1}{2}\sum_{k=-N}^{N} a_k(\mu_i)\cos(kx) + b_k(\mu_i)\sin(kx),$$

where $a_k(\mu_i)$ and $b_k(\mu_i)$ are Fourier coefficients of $P(\mu_i|x)$. We thus find

$$P(\mu_1, \mu_2|\theta) = \frac{1}{4}\sum_{k=-N}^{N} A_k^{(\eta)}(\mu_1, \mu_2)\cos(k\theta) + B_k^{(\eta)}(\mu_1, \mu_2)\sin(k\theta),$$

where the coefficients are given by

$$A_k^{(\eta)}(\mu_1, \mu_2) = \mathbf{a}^{\mathrm{T}}(\mu_1)\mathbf{C}\cdot\mathbf{a}(\mu_2) + \mathbf{b}^{\mathrm{T}}(\mu_1)\mathbf{S}\cdot\mathbf{b}(\mu_2)$$

and

$$B_k^{(\eta)}(\mu_1, \mu_2) = \mathbf{b}^{\mathrm{T}}(\mu_1)\mathbf{C}\cdot\mathbf{a}(\mu_2) - \mathbf{a}^{\mathrm{T}}(\mu_1)\mathbf{S}\cdot\mathbf{b}(\mu_2),$$

$\mathbf{a}(\mu_i) \equiv (a_{-N}(\mu_i), ..., a_N(\mu_i))$ [and analogous definition for $\mathbf{b}(\mu_i)$] are vectors of Fourier coefficients, and the matrices $\mathbf{C}$ and $\mathbf{S}$ have components

$$\mathbf{C}_{k,k'} \equiv \int_0^{2\pi} d\epsilon\, P(\epsilon)\cos(k\epsilon)\cos(k'\epsilon), \qquad \mathbf{S}_{k,k'} \equiv \int_0^{2\pi} d\epsilon\, P(\epsilon)\cos(k\epsilon)\sin(k'\epsilon),$$

respectively. Thus, from the knowledge of the Fourier expansion of the conditional probabilities of the single interferometer, we can directly find the Fourier expansion of the conditional probability of the differential measurement. An advantage of this method is that taking the derivative of $P(\mu_1, \mu_2|\theta)$ from Eq. (D.2), necessary to calculate the FI, is immediate.

References

[1] A.D. Cronin, J. Schmiedmayer and D.E. Pritchard Rev. Mod. Phys. **81**, 1051 (2009).

[2] A. Peters, K.Y. Chung and S. Chu, Nature **400**, 849-852 (1999).

[3] T.L. Gustavson, P. Bouyer and M.A. Kasevich, Phys. Rev. Lett. **78**, 2046 (1997); M. Fattori, et al., Phys. Rev. Lett. **100**, 080405 (2008).

[4] C.R. Ekstrom, et al., Phys. Rev. A **51**, 3883 (1995).

[5] R. Bouchendira, et al., Phys. Rev. Lett. **106**, 080801 (2011).

[6] J.K. Stockton, X. Wu and M.A. Kasevich, Phys. Rev. A **76**, 033613 (2007).
[7] D. S. Durfee, Y.K. Shaham and M.A. Kasevich, Phys. Rev. Lett. **97**, 240801 (2006); A. Gauguet, et al., Phys. Rev. A **80**, 063604 (2009).
[8] M.J. Snadden, et al., Phys. Rev. Lett. **81**, 971 (1998).
[9] J.B. Fixler, et al., Science **5**, 74 (2007); G. Lamporesi, et al., Phys. Rev. Lett. **100**, 050801 (2008)
[10] S. Dimopoulos, et al., Phys. Rev. Lett. **98**, 111102 (2007); G. Varoquaux, et al., New J. of Phys. **11**, 113010 (2009).
[11] S. Fray, et al., Phys. Rev. Lett. **93**, 240404 (2004); J.M. Hogan, D.M. S. Johnson and M.A. Kasevich, in Proc. of the Int. School of Phys. Enrico Fermi on Atom Optics and Space Physics, edited by E. Arimondo, W. Ertmer and W.P. Schleich (IOS Press, Amsterdam, 2009) pp. 411-447, arXiv:0806.3261.
[12] A. Arvanitaki, et al., Phys. Rev. Lett. **100**, 120407 (2008).
[13] S. Dimopoulos, et al., Phys. Rev. D **78**, 122002 (2008).
[14] A. Sørensen, et al., Nature **409**, 63 (2001).
[15] V. Giovannetti, S. Lloyd and L. Maccone, Phys. Rev. Lett.**96**, 010401 (2006).
[16] L. Pezzè and A. Smerzi, Phys. Rev. Lett. **102**, 100401 (2009).
[17] P. Hyllus, et al., Phys. Rev. A **85**, 022321 (2012); G. Tòth, Phys. Rev. A **85**, 022322 (2012).
[18] J. Appel, et al., PNAS **106**, 10960 (2009); M.H. Schleier-Smith, et al., Phys. Rev. Lett. **104**, 073604 (2010); Z. Chen, et al., Phys. Rev. Lett. **106**, 133601 (2011); R. J. Sewell, et al., Phys. Rev. Lett. **109**, 253605 (2012).
[19] J. Estéve, et al., Nature **455**, 1216 (2008).
[20] C. Gross, et al., Nature **464**, 1165 (2010); M. F. Riedel, et al., Nature **464**, 1170 (2010).
[21] B. Lücke, et al., Science **334**, 773 (2011).
[22] T. Berrada, et al., Nat. Commun. **4**, 2077 (2013).
[23] C.F. Ockeloen, et al., Phys. Rev. Lett. **111**, 143001 (2013).
[24] H. Strobel, et al., Science **345**, 6195 (2014).
[25] S.F. Huelga, et al., Phys. Rev. Lett. **79**, 3865 (1997).
[26] A. Shaji and C.M. Caves, Phys. Rev. A **76**, 032111 (2007).
[27] B.M. Escher, R.L. de Matos Filho and L. Davidovich, Nat. Phys. **7**, 406 (2011).
[28] R. Demkowicz-Dobrzanski, J. Kolodynski and M. Guta, Nat. Comm. **3**, 1063 (2012).
[29] A.W. Chin, S.F. Huelga and M.B. Plenio, Phys. Rev. Lett. **109**, 233601 (2012); P. Szankowski, J. Chwedenczuk, M. Trippenbach, arXiv:1212.2528.
[30] Quantum-enhanced noiseless differential interferometry is studied in K. Eckert, et al., Phys. Rev. A **73**, 013814 (2006).
[31] An optical analogous to the differential scheme discussed here (a differential Michelson-Morley interferometer with squeezed states of light as input, in particular) has been recently investigated in I. Ruo Bouchera, I. P. Degiovanni, S. Olivares and M. Genovese, Phys. Rev. Lett. **24**, 213601 (2013). See also noise quenching in correlated-emission laser, originally proposed in M.O. Scully, Phys. Rev. Lett. **55**, 2802 (1985) and experimentally demonstrated in M. Winters, J. Hall and P.E. Toschek, Phys. Rev. Lett. **65**, 3116 (1990).
[32] H. Cramér, *Mathematical Methods of Statistics* (Princeton Univ. Press, Princeton, NJ, 1946).
[33] S.L. Braunstein and C.M. Caves, Phys. Rev. Lett. **72**, 3439 (1994).
[34] C.W. Helstrom, *Quantum Detection and Estimation Theory* (Academic, 1976).
[35] The concept of DFS for general quantum information proposes was introduced in [36] and experimentally investigated in [37].
[36] P. Zanardi and M. Rasetti, Phys. Rev. Lett. **79**, 3306 (1997); L.M. Duan and G.C. Guo, Phys. Rev. Lett. **79**, 1953 (1997); D.A. Lidar, I.L. Chuang and K.B. Whaley, Phys. Rev. Lett. **81**, 2594 (1998).
[37] P. Kwiat, et al., Science **290**, 498 (2000); D. Kielpinski, et al., Science **291**, 1013 (2001).
[38] C.F. Roos, et al., Nature **443**, 316 (2006).
[39] T. Monz, et al., Phys. Rev. Lett. **106**, 130506 (2011).

[40] U. Dorner, New J. Phys. **14**, 043011 (2012).
[41] J.J. Bollinger et al., Phys. Rev. A **54**, R4649 (1996); H. Lee, P. Kok and J.P. Dowling, J. Mod. Opt. **49**, 2325 (2002).
[42] M.J. Steel and M.J. Collett, Phys. Rev. A **57**, 2920 (1998); J. Javanainen and M.Y. Ivanov, Phys. Rev. A **60**, 2351 (1999).
[43] L. Pezzè and A. Smerzi, Phys. Rev. Lett. **1**10, 163604 (2013).
[44] L. Pezzè, et al., Phys. Rev. A **72**, 043612 (2005).
[45] M. Kitagawa and M. Ueda, Phys. Rev. A **47**, 5138 (1993).
[46] For the effect of phase noise in the state preparation see G. Ferrini, et al., Phys. Rev. A **82**, 033621 (2010).